JOURNAL OF CATALYSIS 155, 82–94 (1995)

Oxidative Dehydrogenation of Isobutane over Monoliths at Short Contact Times

Marylin Huff[1] and Lanny D. Schmidt[2]

Department of Chemical Engineering and Materials Science, University of Minnesota, Minneapolis, Minnesota 55455

Received December 6, 1994; revised April 12, 1995

Isobutylene can be produced with high selectivity and conversion by oxidative dehydrogenation of isobutane in air or oxygen over a ceramic foam monolith coated with Pt at contact times of ~5 ms in an atmospheric pressure reactor operating at 800 to 900° C. Total olefin selectivities up to 80% (40% isobutylene, 40% propylene) at 60% conversion of isobutane are achieved in an autothermal process with higher reactant conversion when the reactants are preheated up to 400°C. No carbon build-up is observed at molar isobutane-to-oxygen feed ratios up to 2.5, and the catalyst shows no deactivation over at least several weeks of operation.

Maximum isobutylene selectivity occurs at a fuel-to-oxygen ratio of 1.4 at contact times ≤5 ms, while propylene yield is maximized at longer contact times and at higher fuel-to-oxygen ratios. The total selectivity to methane, ethane, and ethylene is always much less than the total selectivity to isobutylene and propylene.

A simple reaction mechanism can explain these products. Surface oxygen abstracts a hydrogen from isobutane resulting in an isobutyl group on the surface. On the Pt surface, β-elimination reactions than take place, leading to either isobutylene or propylene production. The small amounts of smaller hydrocarbons compared to *n*-butane oxidation or to homogeneous cracking are explained by the absence of a β-alkyl group on the isobutyl species adsorbed at a 3° carbon.

INTRODUCTION

Isobutylene, the key reactant for MTBE production for gasoline oxygenates, is typically produced industrially by the endothermic dehydrogenation of isobutane over a Cr_2O_7–Al_2O_3 catalyst near 900 K (1) with a catalyst contact time near 1 s:

$$i\text{-}C_4H_{10} \rightarrow i\text{-}C_4H_8 + H_2. \qquad [1]$$

Although the selectivity to isobutylene is nearly 100%, the isobutane-per-pass conversion is less than 5%. However, at an isobutane conversion of 80%, the isobutylene selectivity falls to less than 20% in a similar reactor (2). This process has the additional problem that carbon deposition often leads to catalyst deactivation and the consequent need for periodic catalyst regeneration in air. Because of the industrial relevance of isobutylene production, much of the research done in this area is covered in the patent literature (3–6).

Several research groups are pursuing ways to improve the isobutylene yield, catalyst stability, and process economics. Researchers at Phillips Petroleum Company have investigated the addition of steam to reduce the problem of carbon deposition (3–5):

$$C_S + H_2O \rightarrow CO + H_2. \qquad [2]$$

The reactor is periodically purged so that the catalyst can be regenerated in an oxygen and steam atmosphere and finally reactivated in a reducing atmosphere (3). This process can yield 45% isobutylene per pass (4).

Researchers at Shell International have also developed a unique reactor design that leads to 51% isobutylene yield ($S_{iC_4H_8}$ × Conversion) using a cross-flow moving bed reactor where the catalyst particles are supported on a gas permeable conveyer. The isobutane is introduced through the porous bottom of the reactor and the product gases are collected above the catalyst particles. This moving bed approach allows the catalyst to be continuously regenerated.

Membrane reactors have been studied as a possible means to exceed the equilibrium limitation in the isobutane dehydrogenation reaction (1) (Eq. [1]). A Pd membrane reactor is loaded with a packed bed of catalyst, often Pt/Al_2O_3 or Cr_2O_7/Al_2O_3. The H_2 produced by the dehydrogenation reaction passes through the Pd membrane and leaves the reaction zone. This approach does not improve the isobutylene yield and carbon deposition is still a problem; however, by removing the hydrogen the isobutylene selectivity increases, since the hydroisomerization

$$i\text{-}C_4H_8 + H_2 \rightarrow n\text{-}C_4H_8 + H_2 \qquad [3]$$

---

[1] Current address: Department of Chemical Engineering, University of Delaware, Newark DE 19716.

[2] To whom correspondence should be addressed.

0021-9517/95 $12.00

and hydrogenolysis

$$i\text{-}C_4H_8 + H_2 \rightarrow C_3H_6 + CH_4 \qquad [4]$$

reactions can no longer occur.

Other researchers have studied the effect of the catalyst support on the dehydrogenation process (7). Chromia supported on Al_2O_3, SiO_2, and ZrO_2 have all been compared. It has been suggested that lattice oxygen plays a necessary role in the dehydrogenation reaction. The ZrO_2 support yields the highest catalytic activity with an initial isobutane conversion of 40% (with nearly 100% selectivity to isobutylene), but the catalyst quickly deactivates due to carbon deposition and lattice oxygen depletion, and the conversion drops to less than 5% within the first two hours of operation.

By adding oxygen to the feed, the production costs can be greatly reduced since the oxidative dehydrogenation of isobutane is exothermic:

$$i\text{-}C_4H_{10} + \tfrac{1}{2}\,O_2 \rightarrow i\text{-}C_4H_8 + H_2O. \qquad [5]$$

This concept has been applied using several pyrophosphate catalysts (8). Isobutylene can be produced with 82% selectivity at ~10% isobutane conversion over $Ni_2P_2O_7$ at 550°C.

We have recently reported very high yields of olefins from ethane (9), propane, or *n*-butane (10) by catalytic oxidative dehydrogenation over Pt-coated monoliths at very short contact times. Olefin selectivities up to 70% at conversions better than 80% have been achieved with a catalyst contact time <5 ms. This short contact time and autothermal operation allows for the use of much smaller reactors with very low operating costs. Researchers at British Petroleum have reported similar results primarily using straight-channel honeycomb monoliths (11). The foam monoliths lead to more turbulent flow patterns in the catalyst channels and somewhat better product yields with smaller reaction times.

In this paper, we apply oxidative dehydrogenation over Pt-coated monoliths to the oxidative dehydrogenation of isobutane to isobutylene. The possible reactions of isobutane are listed in Table 1 with their corresponding heats of reaction and equilibrium constants. Isobutylene can be formed by either oxidative dehydrogenation (Eq. [5]) or thermal dehydrogenation (Eq. [1]). However, in the presence of O_2 the isobutane can be combusted,

$$i\text{-}C_4H_{10} + \tfrac{13}{2}\,O_2 \rightarrow 4CO_2 + 5H_2O \qquad [6]$$

or partially oxidized to syngas,

$$i\text{-}C_4H_{10} + 2O_2 \rightarrow 4CO + 5H_2. \qquad [7]$$

These reactions are quite exothermic and provide the heat required for endothermic cracking reactions including isobutane cracking,

$$i\text{-}C_4H_{10} \rightarrow C_3H_6 + CH_4, \qquad [8]$$

and product olefin cracking,

$$i\text{-}C_4H_8 \rightarrow 4C_S + 4H_2 \qquad [9]$$

$$C_3H_6 \rightarrow 3C_S + 3H_2. \qquad [10]$$

These carbon-forming reactions are listed in Table 2.

The objective of this research is to apply this catalyst structure to the production of isobutylene to determine under what reaction conditions isobutylene production can be maximized. We also examine the effects of metal loading and the effects of the catalyst support by using both α-Al_2O_3 and ZrO_2 foam monoliths. We also discuss briefly the effects of the addition of Au.

TABLE 1

Reactions of Isobutane

	% fuel in air	ΔT_{ad} (°C)	fuel/O_2	$\Delta H°$ (kJ/mol)	K_{eq} 1200 K
$i\text{-}C_4H_{10} + \tfrac{13}{2}O_2 \rightarrow 4CO_2 + 5H_2O$ complete combustion	3.1	2709	0.15	−2650	$>10^{38}$
$i\text{-}C_4H_{10} + 2O_2 \rightarrow 4CO + 5H_2$ partial oxidation to syngas	9.5	928	0.50	−310	$>10^{38}$
$i\text{-}C_4H_{10} + \tfrac{1}{2}O_2 \rightarrow i\text{-}C_4H_8 + H_2O$ oxidative dehydrogenation	29.6	811	2.00	−103	1.1×10^{10}
$i\text{-}C_4H_{10} \rightarrow i\text{-}C_4H_8 + H_2$ dehydrogenation	—	—	—	+139	1.4×10^{2}
$i\text{-}C_4H_{10} \rightarrow C_3H_6 + CH_4$ cracking	—	—	—	+76	5.5×10^{4}

TABLE 2

Reactions Producing Solid Carbon

	ΔH° (kJ/mol)	K_{eq} 1200 K	K_{exp} 1200 K
$i\text{-}C_4H_8 \rightarrow 4C_S + 4H_2$ cracking	+133	7.1×10^{13}	5.2×10^{-5}
$C_3H_6 \rightarrow 3C_S + 3H_2$ cracking	−20	2.9×10^{9}	8.5×10^{-4}
$C_2H_4 \rightarrow 2C_S + 2H_2$ cracking	−53	9×10^{5}	1.2×10^{-1}
$2CO \rightarrow C_S + CO_2$ CO disproportionation (Boudouard)	−172	1.7×10^{-2}	14.2
$CO + H_2 \rightarrow C_S + H_2O$ reverse steam reforming of carbon	−131	2.5×10^{-2}	104

EXPERIMENTAL

The reactor and experimental apparatus have been described previously for the partial oxidation of methane (12), oxidative dehydrogenation of ethane (9), and oxidative dehydrogenation and cracking of propane and butane (10).

The catalysts are prepared by depositing Pt or a mixture of Pt and Au on commercially available ceramic foam monoliths. The foam monoliths, obtained from Hi-Tech Ceramics, are either α-Al_2O_3 or ZrO_2 with 45 pores per linear inch (ppi). It is important to note that these catalysts are not microporous structures. The monoliths are not wash-coated and are estimated to have a surface area of less than 70 cm^2/g.

Pt is deposited on the ceramic by impregnating the monolith with a saturated solution of H_2PtCl_6 in water. The monolith is then dried in N_2, calcined in air, and reduced in H_2. This process leads to 3–6 wt.% Pt loading for α-Al_2O_3 and 1–2 wt.% Pt loading for ZrO_2 per impregnation step. Higher loadings were achieved by repeating this process. The Pt–Au/α-Al_2O_3 catalyst was prepared by impregnating a Pt/α-Al_2O_3 monolith with a warm saturated solution of $AuCl_3$ in water. Due to the low solubility of $AuCl_3$ in water, the impregnation and drying steps were repeated thrice before calcination and reduction. This led to a 2.8 wt.% Au–3.6 wt.% Pt/α-Al_2O_3 catalyst.

The gas flow rates into the reactor were controlled by mass flow controllers with accuracies of 0.1 SLPM for all gases. In separate experiments, we have measured the pressure drop through the catalyst at the flow rates and temperatures used here and found the pressure drop to be <0.10 psi. The product compositions were measured at steady state by GC analysis as discussed in detail elsewhere (12). Individual species concentrations were measured with reproducibility within ±2%. It is also important to note that a rigorous analysis of the products led to closure of the material balances to within 4%. Some minor products, primarily C_2H_6 and C_3H_8, which were formed with less than 1% selectivity are not discussed here explicitly.

The data presented consist of selectivities, conversion, and reaction temperature. The selectivities for carbon-containing species are computed on a carbon atom basis, and the H_2 and H_2O selectivities are calculated on a hydrogen atom basis. This method implicitly accounts for the mole number change due to reaction. The conversion is calculated on both a fuel and an oxygen basis. The conversion calculated on the i-C_4H_{10} basis parallels the previous work with other alkanes (9, 10). For these other fuels, the oxygen was always completely consumed. In the isobutane oxidation experiments, however, the oxygen is no longer completely consumed but is a fairly minor component in the product stream.

RESULTS

The bulk of the data presented here is for the oxidative dehydrogenation of isobutane over a 5.1 wt.% Pt/α-Al_2O_3 foam monolith catalyst. We describe product variations with reactant composition, reaction temperature, and catalyst contact time. We also report the results over a slightly more active 1.8 wt.% Pt/ZrO_2 catalyst and discuss the effects of Pt loading and the addition of Au to the Pt/α-Al_2O_3 catalyst. We attempted experiments using blank α-Al_2O_3 and ZrO_2 monoliths. Even when externally heating these monoliths to ~600°C, no significant conversion was achieved.

Air oxidation. Figure 1 shows the carbon atom and hydrogen atom selectivities, conversion, and the reaction temperature for the oxidation of isobutane in air over a 5.1 wt.% Pt/α-Al_2O_3 catalyst as a function of the fuel/O_2 ratio in the feed. The relative amounts of isobutane and air were adjusted while maintaining a constant total feed flow rate of 5 SLPM with room temperature feed.

Experiments were conducted on the stoichiometric fuel/O_2 ratios for the production of syngas (Eq. [7]) and for oxidative dehydrogenation (Eq. [5]) as indicated in Table 1. Experiments were not conducted at fuel/O_2 ratios less than 0.5 due to the flammability of these mixtures. If only oxidation reactions were occurring, one would expect production to shift from CO and H_2 at the leaner compositions to isobutylene and H_2O at the richer compositions. Figure 1 indeed exhibits this trend. The reaction temperature is also near the adiabatic reaction temperatures listed in Table 1 for these reactions.

Several other reactions, including thermal dehydrogenation (Eq. [1]) and cracking (Eq. [8]) are also taking place. This somewhat masks the trend described in the

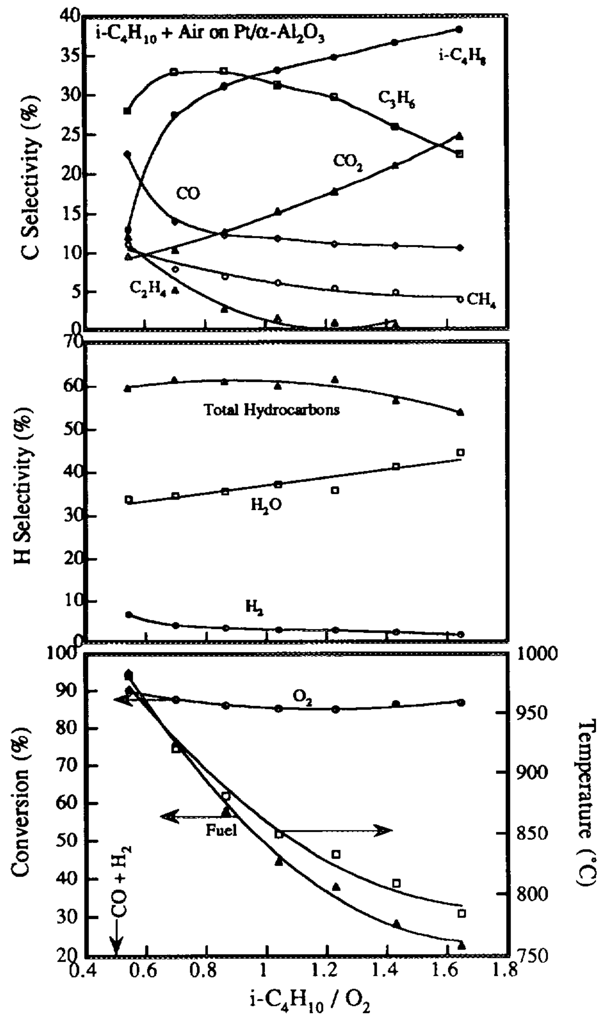

FIG. 1. Carbon selectivity, hydrogen selectivity, conversion, and reaction temperature for *i*-butane oxidation in air over a 5.1 wt.% Pt/α-Al_2O_3 catalyst as a function of the *i*-C_4H_{10}/O_2 ratio in the feed at a total feed flow rate of 5 SLPM in an autothermal reactor at a pressure of 1.4 atm.

previous paragraph. Syngas production is suppressed in favor of thermal cracking to form C_3H_6 and CH_4 (Eq. [8]). The production of CO_2 also increases at richer compositions contrary to the suggested reactions in Table 1. The oxygen is not completely consumed (85–90% O_2 conversion) but is present in only small quantities. This remaining O_2 may lead to the higher CO_2 selectivities achieved in *i*-C_4H_{10} oxidation compared to those in *n*-C_4H_{10} oxidation (10).

For isobutane oxidation in air, the production shifts from 33% selectivity to C_3H_6 with 80% isobutane conversion at a fuel/O_2 ratio of 0.7 to 38% selectivity to *i*-C_4H_8 with only 25% isobutane conversion at a fuel/O_2 ratio of 1.65. Throughout this composition region, the total olefin selectivity ($S_{i\text{-}C_4H_{10}} + S_{C_3H_6} + S_{C_2H_4}$) remains high and fairly constant at ~60%. It is informative to notice that the selectivities to C_3H_6 and CH_4 are present in a nearly 3 : 1 ratio. Since the selectivities are calculated on a carbon atom basis, this corresponds to one mole of C_3H_6 for every mole of CH_4, supporting the unimolecular cracking reaction (Eq. [8]).

Preheat. Figure 2 shows the carbon atom and hydrogen atom selectivities, conversion, and reaction temperature for isobutane oxidation in air over a 5.1 wt.% Pt/α-Al_2O_3 catalyst where the reactants have been preheated to 360°C prior to reaching the catalytic zone. Data are presented as a function of the fuel/O_2 ratio in the feed.

Figure 2 shows a substantial increase in reaction temperature and isobutane conversion compared to the

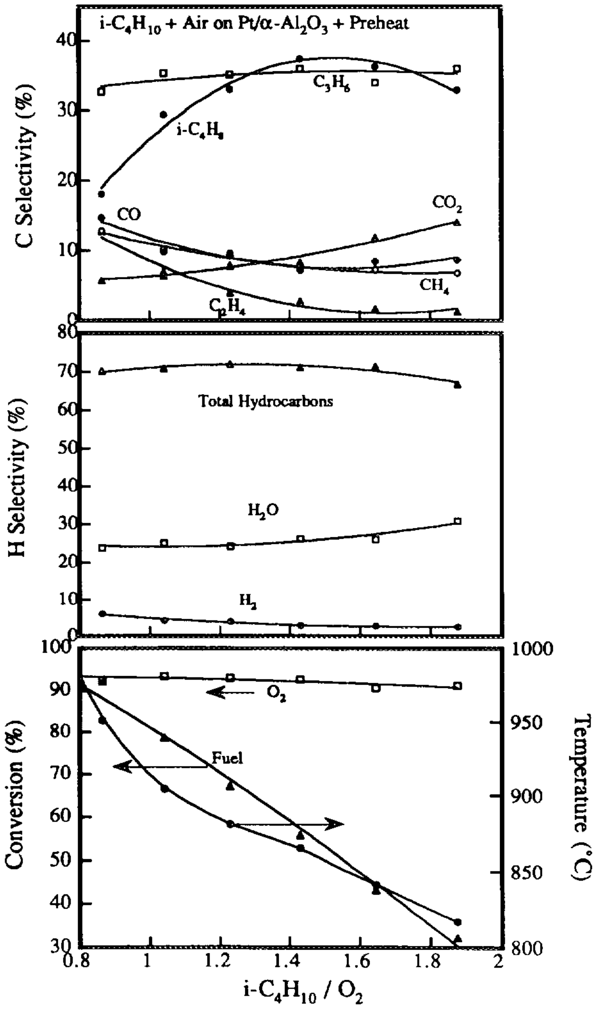

FIG. 2. Selectivity, conversion, and reaction temperature for *i*-butane oxidation in air over a 5.1 wt.% Pt/α-Al_2O_3 catalyst as a function of the fuel/O_2 ratio in the feed at a total feed flow rate of 5 SLPM at a pressure of 1.4 atm. The reactants have been preheated to 360°C prior to reaching the catalytic zone.

results shown in Fig. 1, while the selectivity distribution changes little. The reaction temperature is ~50°C hotter when the preheat is utilized. At a fuel/O_2 ratio of 1.65, the isobutylene selectivity is 37%, nearly the same as it was without preheat, and the C_3H_6 selectivity has risen from 22% without preheat to 35% with 360°C preheat. The O_2 conversion is also somewhat higher at about 94%. The major improvement, however, is the increase in isobutane conversion from 25% to 45% accompanied by an increase in the total olefin selectivity.

Oxidation in O_2. In Figure 3 we show the effect of a reduction in the amount of N_2 diluent present in the reactant stream. The reactants, isobutane and O_2 (with 20% N_2 present for GC calibration), are preheated to 360°C prior to reaching the catalytic zone. Figure 3 shows another substantial increase in the isobutane conversion while there is no significant decrease in isobutylene selectivity. At a fuel/O_2 ratio of 1.65, the isobutane conversion in now 75% with an isobutylene selectivity of 35%. The O_2 conversion has also increased from 95 to 98%. The reaction temperatures indicated here agree well with the values shown in Fig. 2. The selectivity to isobutylene is nearly 45% at the stoichiometric ratio for oxidative dehydrogenation (fuel/O_2 = 2.0), while the conversion is still greater than 50%.

Flow rate. Figure 4 illustrates the effect of reducing the catalyst contact time by increasing the reactant flow

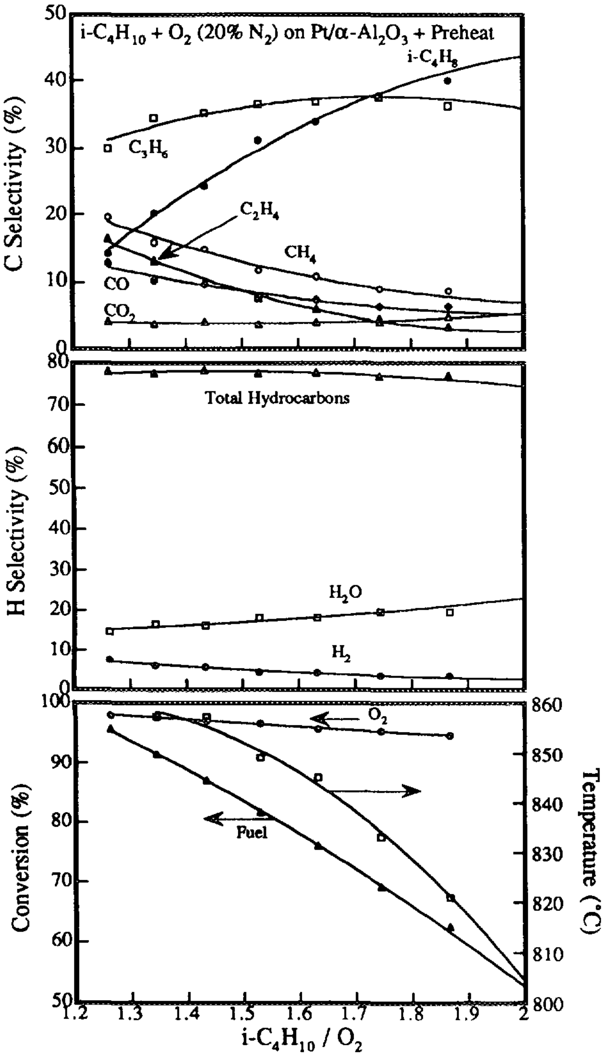

FIG. 3. Selectivities and conversion for *i*-butane oxidation in O_2 (20% N_2 diluent) over a 5.1 wt.% Pt/α-Al_2O_3 catalyst as a function of the fuel/O_2 ratio at a total flow rate of 5 SLPM at a pressure of 1.4 atm. The reactants have been preheated to 360°C prior to reaching the catalytic zone.

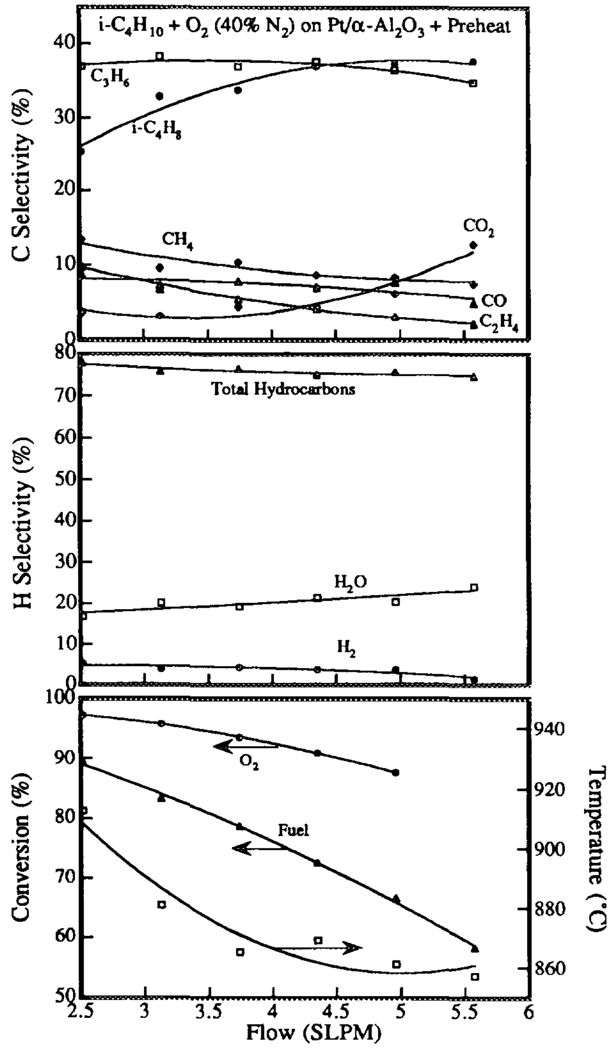

FIG. 4. Selectivities and conversion for *i*-butane oxidation in O_2 (40% N_2 diluent) over a 5.1 wt.% Pt/α-Al_2O_3 catalyst at a fuel/O_2 ratio of 1.43 as a function of flow rate at a pressure of 1.4 atm. The reactants have been preheated to 300°C prior to reaching the catalytic zone.

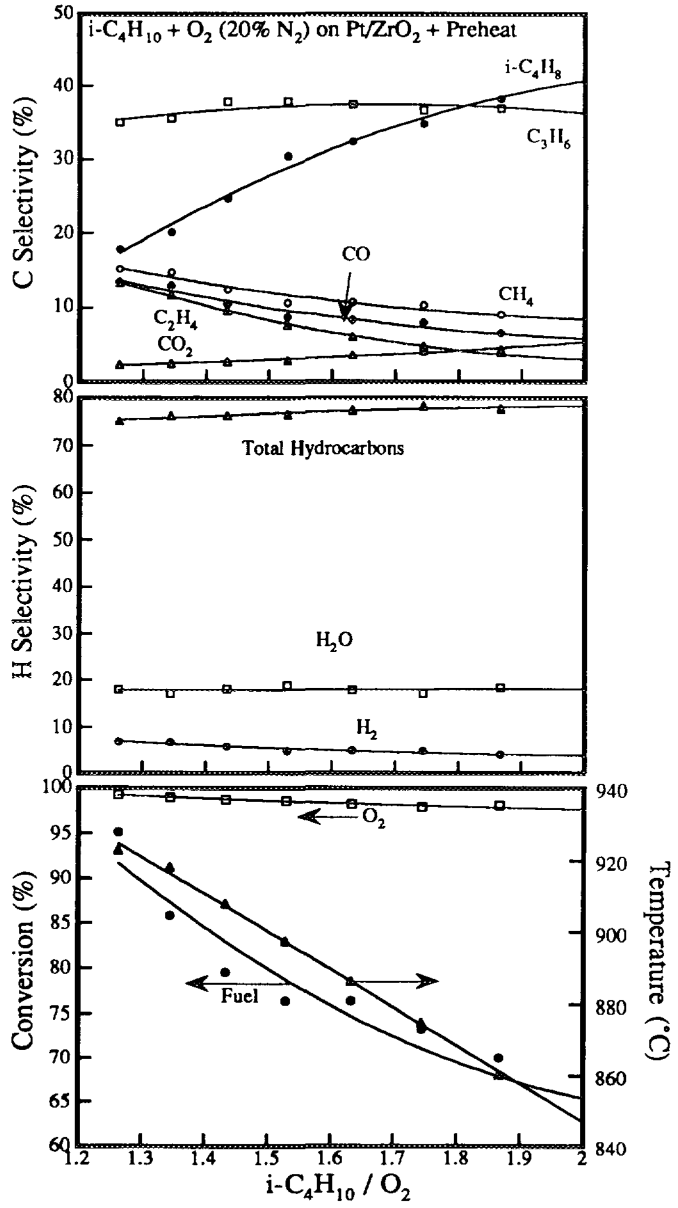

FIG. 5. Selectivity, conversion, and reaction temperature for *i*-butane oxidation in O_2 (20% N_2 diluent) over a 1.8 wt.% Pt/ZrO_2 catalyst as a function of the fuel/O_2 ratio at a total flow rate of 5 SLPM at a pressure of 1.4 atm. The reactants have been preheated to 360°C prior to reaching the catalytic zone.

TABLE 3

Comparison of Various Catalysts for $i - C_4H_{10}$ Oxidation in O_2 (20% N_2 Diluent) at a Total Flow Rate of 5 SLPM with 360°C Reactant Preheat

Catalyst	5.1 wt.% Pt/Al_2O_3	1.8 wt.% Pt/ZrO_2	2.6 wt.% Pt/ZrO_2
i-C_4H_{10}/O_2	2.00	2.00	2.00
Conversion	52	62	55
S_{Olefins}	83	80	81
$S_{i\text{-}C_4H_8}$	45	41	42
$S_{C_3H_6}$	36	36	36
Y_{Olefins}	43	50	45
$Y_{i\text{-}C_4H_8}$	23	25	23
$Y_{C_3H_6}$	19	22	20

rate on the selectivities, isobutane conversion, and reaction temperature. These experiments were conducted at a fixed fuel/O_2 ratio of 1.43 since this is the composition at which the optimum total olefin yield is obtained. The reactants were preheated to 300°C prior to reaching the catalytic zone and only 40% N_2 diluent was present.

The isobutane conversion decreases dramatically with flow rate from 90% at 2.5 SLPM to 60% at 5.5 SLPM. The O_2 conversion also decreases slightly with increasing flow rate from 97 to 88%. The reaction temperature at 5 SLPM agrees well with the reaction temperature indicated in Fig. 3 at a fuel/O_2 ratio of 1.43. The reaction temperature is much higher at the lower flow rates and steadily decreases as the conversion decreases. The isobutylene selectivity increased from 25% to 37% and the CO_2 selectivity increased from 4% to 13%. The rest of the selectivities varied little with flow rate.

Alternate catalysts. Figure 5 shows the effect of the catalyst support on the selectivities, isobutane conversion, and reaction temperature. Isobutane and O_2 (with 20% N_2 diluent) are preheated to 360°C prior to passing over the 1.8 wt.% Pt/ZrO_2 catalyst. The data shown in Fig. 5 parallel the data shown in Fig. 3 for the $Pt/\alpha\text{-}Al_2O_3$ catalyst.

The reaction temperature over the Pt/ZrO_2 catalysts is higher than the reaction temperature over the $Pt/\alpha\text{-}Al_2O_3$ catalyst by ~50–80°C. The conversions in Fig. 5 are

TABLE 4

Comparison of Various Catalysts for $i - C_4H_{10}$ Oxidation in O_2 (20% N_2 Diluent) at a Total Flow Rate of 5 SLPM with 360°C Reactant Preheat

Catalyst	5.1 wt.% Pt/Al_2O_3	1.8 wt.% Pt/ZrO_2	2.6 wt.% Pt/ZrO_2
i-C_4H_{10}/O_2	1.43	1.43	1.43
Conversion	75	87	85
S_{Olefins}	75	72	76
$S_{i\text{-}C_4H_8}$	33	25	30
$S_{C_3H_6}$	36	38	38
Y_{Olefins}	56	63	65
$Y_{i\text{-}C_4H_8}$	25	22	26
$Y_{C_3H_6}$	27	33	33

slightly higher than those shown in Fig. 3. Slightly less CH_4 is produced over the ZrO_2 support. The olefin selectivity and yield results are summarized in Table 3 for a fuel–O_2 ratio of 2.00 and in Table 4 for a fuel/O_2 ratio of 1.43. The olefin selectivities decrease slightly over the Pt/ZrO_2 catalyst, but the increased conversion leads to a better total olefin yield.

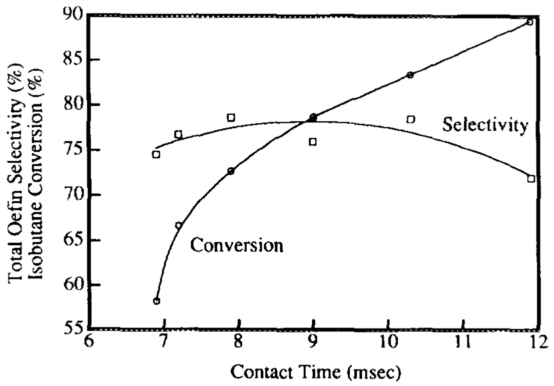

FIG. 6. Isobutane conversion and total olefin selectivity as a function of the catalyst contact time for *i*-butane oxidation in O_2 (40% N_2 diluent) over a 5.1 wt.% Pt/α-Al_2O_3 catalyst at a fuel/O_2 ratio of 1.43 at a pressure of 1.4 atm. The reactants have been preheated to 300°C prior to reaching the catalytic zone.

Tables 3 and 4 also list the results for a higher loading of 2.6 wt.% Pt/ZrO_2 catalyst. The increase in loading shows very little effect on the product selectivities and only a slight decrease in isobutane conversion. When a 2.8 wt.% Au–3.6 wt.% Pt/α-Al_2O_3 catalyst was tested, the catalyst lacked sufficient activity to sustain the reaction, and no reaction products were observed.

DISCUSSION

The dominant features of these experiments include the following:

(1) Carbon deposition is not observed although thermodynamics predicts it, and other research groups report heavy coking under nonoxidative (1, 7), oxidative (11), and steam cracking (5) reaction conditions.

(2) We achieve olefin yields better than the best industrial yields (3, 6) in a much smaller and simpler reactor. Our isobutylene yields are within a factor of two of the best industrial yields (3, 6). The catalyst contact time is 50–100 times smaller over the monolith than in typical industrial processes.

(3) Increasing the reaction temperature, either by adding reactant preheat or by removing N_2 diluent, drastically increases the isobutane conversion without a significant loss in isobutylene selectivity. The propylene selectivity actually increases at elevated temperatures.

(4) The isobutane conversion increases with increasing catalyst contact time as shown in Fig. 6. The total olefin selectivity is fairly independent of contact time while the isobutylene selectivity increases at lower contact times.

(5) The Pt/ZrO_2 catalyst shows a slightly higher activity than the Pt/α-Al_2O_3 catalyst, but Pt loading does not seem to have a major effect on the catalyst activity or product distribution. The addition of 2.8 wt.% Au to the 3.6 wt.% Pt/α-Al_2O_3 catalyst led to no catalytic activity.

A mechanism similar to the ones proposed for ethane, propane, and *n*-butane oxidative dehydrogenation (9, 10) can also be applied to isobutane. In the following sections, we will detail this mechanism and address the issues outlined above. However, there are aspects of the isobutane system that differ dramatically from the previously studied systems:

(1) In ethane, propane, and *n*-butane oxidative dehydrogenation, the oxygen was always completely consumed (9, 10). This is not the case in the isobutane system.

(2) Alkane conversions are significantly lower for isobutane oxidation than they were for *n*-butane oxidation (10) under similar reaction conditions. We believe that the reaction steps shown in Fig. 7 and the discussion that follows can accurately account for these observations.

Competing Mechanisms

There are several possible reaction mechanisms that can lead to olefin production under these reaction conditions. Olefins can be formed homogeneously (2) or heterogeneously on a metal surface (1) or an oxide surface (7,

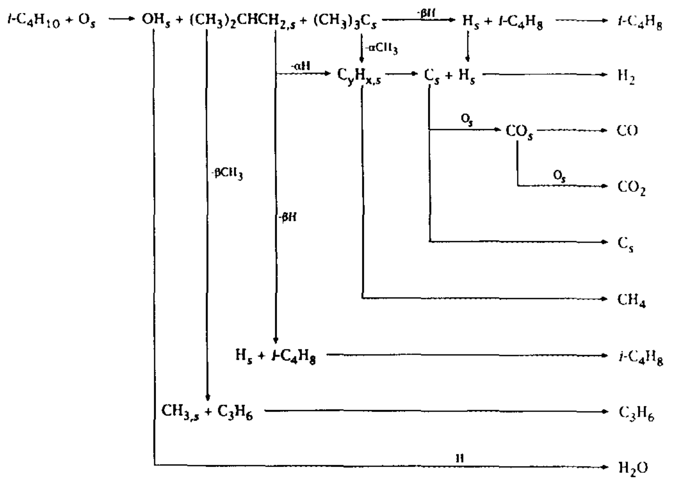

FIG. 7. Proposed surface reactions for isobutane oxidation over a supported Pt catalyst. The gaseous species produced are indicated at the far right.

8) in the presence (8, 13) or absence (7) of free oxygen. We discuss characteristics of each of these mechanisms in the following paragraphs and suggest the relative importance of each of these mechanisms in the present research.

Thermal pyrolysis. In accord with previous discussion for other alkane oxidative dehydrogenation systems (9, 10), we do not believe that a pyrolysis mechanism can explain the products observed here. The product distribution achieved in thermal pyrolysis (2) is listed in Table 5 and is compared to the product distribution obtained in this work at the same level of isobutane conversion.

Pyrolysis involves gas phase free radical reactions which lead to significant production of acetylene, butadiene, and aromatics (~11% on a carbon atom basis) (2). Looking at Table 5, we do not observe significant production of any of these compounds. However, we obtain much higher selectivities to isobutylene and propylene than are obtained in industrial pyrolysis with a considerably shorter reaction time. Of course, the presence of oxygen in this system will affect the product distribution. In propane pyrolysis (14), the presence of oxygen has been linked to higher olefin yields and less production of aromatics. However, even in the presence of oxygen the hydrocarbon conversion was only 20% with a residence time of ~4 s at 700°C. In the reactor discussed here, the hydrocarbon conversion is much higher at 800–1000°C with a residence time of only 5–10 ms.

The conversion thus appears to be much too high for homogeneous reactions or thermal pyrolysis alone to explain. In the absence of oxygen, the product distribution would reflect a more significant aromatic and more deeply unsaturated hydrocarbon component. In cases where the reactants have been preheated prior to reaching the catalyst, the reactant temperature is ramped to the designated preheat temperature from room temperature over the course of <0.5 s. The designated preheat temperature is the maximum gas temperature measured immediately before entering the catalyst. It is unlikely that the reactants are hot enough for a long enough period of time prior to reaching the catalyst for a significant contribution through the relatively slow homogeneous reactions to develop. Blank experiments in which the reactants were heated to 600°C with no Pt gave essentially zero conversion.

TABLE 5

Comparison of Product Distribution for Pyrolysis of Isobutane and Oxidative Dehydrogenation of Isobutane on a Carbon Atom Basis at 80% Isobutane Conversion

	Pyrolysis	Oxidative dehydrogenation
CH_4	15%	11%
C_2H_6, C_3H_8	1%	2%
C_2H_4	6%	6%
C_3H_6	27%	38%
i-C_4H_8	20%	31%
C_2H_2, C_3H_4, C_4H_6	6%	<0.3%
CO	<0.2%	8%
CO_2	<0.2%	3%
C_5+, Aromatics	5%	<0.2%.
τ	0.3 sec	0.006 sec

Catalytic dehydrogenation. Dehydrogenation of isobutane to isobutylene over oxide catalysts has been studied in detail in the absence of free oxygen. Most research has focused on supported chromia catalysts (7), but supported Pt catalysts have also been investigated (1). These studies have been plagued by rapid catalyst deactivation due to carbon deposition and lattice oxygen depletion.

In isobutane dehydrogenation over supported chromia, it is believed that the active site for the dehydrogenation (Eq. [1]) is a Cr(III) species with an adjacent O^{2-} of the support playing an active role. In this reaction system, isobutane cracking to propylene and methane (Eq. [8]) occurs at a Brønsted acid site on the support. It is suggested that Cr_2O_7–ZrO_2 has a higher activity than Cr_2O_7–Al_2O_3 because there is a higher concentration of Cr(V) species (precursor for Cr(III)) on the ZrO_2 support (7).

In our studies, we observe a similar importance of the dehydrogenation to isobutylene (Eqs [1] and [5]) and cracking to propylene and methane (Eq. [8]) reactions. One use of the oxygen in our system may be the maintenance of catalyst activity by the continuous reoxidation of the oxide support and the removal of coke. However, as we will discuss shortly, we do not believe that activity maintenance is the primary role of oxygen in our system.

Catalytic oxidative dehydrogenation. In oxidative dehydrogenation over vanadate catalysts, the first reaction step on the surface is the formation of an adsorbed alkyl and hydroxyl group (13). The experiments over the vanadate catalysts were conducted in the presence of free oxygen, near the stoichiometries used in this study, but the reactants were diluted in an inert gas (usually He or N_2), so that the inert gas accounted for 85–90% of the gas feed. Although our work differs strongly from this study in the identity of the catalyst (Pt vs V–Mg–O), the level of reactant dilution (20 vs 88%), the reaction temperature (900 vs 500°C), and the contact time (0.005 vs ~0.2), many similarities exist which are discussed in the following sections.

Reaction Steps

The reaction steps for isobutane oxidative dehydrogenation on Pt/α-Al_2O_3 or Pt/ZrO_2 catalysts shown in Fig. 7 can be simplified to five essential steps,

$$\begin{aligned} i\text{-}C_4H_{10} \xrightarrow{r_i} i\text{-}C_4H_{9,S} &\xrightarrow{r_{\beta 3^\circ}} i\text{-}C_4H_8 \\ &\xrightarrow{r_{\beta 1^\circ}} C_3H_6 + CH_4 \qquad [11] \\ &\xrightarrow{r_\alpha} C_S \xrightarrow{r_{CO}} CO, \end{aligned}$$

which lead to isobutylene, propylene, carbon monoxide, or coke.

Initiation. As suggested in the oxidative dehydrogenation of isobutane over oxide catalysts, we also believe that the first step in the reaction mechanism is the abstraction of hydrogen by surface oxygen to form an adsorbed isobutyl group and a hydroxyl,

$$i\text{-}C_4H_{10} + O_S \xrightarrow{r_i} i\text{-}C_4H_{9,S} + OH_S \qquad [12]$$

This step may be occurring on lattice oxygen sites of the support or on oxygen adsorbed on the Pt surface. As discussed for the other alkane oxidative dehydrogenation systems (9, 10), at the initial reaction conditions (P_{O2} = 200 Torr, T = 900°C) the Pt surface is predicted to be completely covered by O_S.

These reactions are carried out in the fuel rich regime, but, unlike the oxidative dehydrogenation of n-butane[10], only 90–95% of the oxygen is consumed in our experiments. This oxygen breakthrough suggests that the rate-limiting initiation step (Eq. [12]) for isobutane oxidative dehydrogenation is much slower than the corresponding initiation step for n-butane oxidative dehydrogenation,

$$n\text{-}C_4H_{10} + O_S \xrightarrow{r_i} C_4H_{9,S} + OH_S \qquad [13]$$

With isobutane, the O_2 conversion decreases with decreasing contact time (increasing flow rate, see Fig. 4) suggesting that oxygen is involved in a relatively slow reaction step, so perhaps hydrogen abstraction by surface oxygen is the rate-limiting step.

The rates of these reactions should be related to the strengths of the C–H bonds that must be broken. The bond energy of a primary (1°), secondary (2°), and tertiary (3°) C–H bond is 410, 395, and 375 kJ/mol, respectively (13). Although isobutane has one 3° C–H bond which is the most easily broken, the remaining nine 1° C–H bonds are much stronger. On the other hand, n-butane has four relatively weak 2° C–H bonds. Coupled with steric effects, this difference leads to the rate of the initiation step for n-butane oxidative dehydrogenation (Eq. [13]) being much faster than the rate of the initiation step for isobutane oxidative dehydrogenation (Eq. [12]). Since r_i is relatively slow, the conversions for isobutane are much smaller than the conversions for n-butane under similar conditions and some oxygen passes through the catalyst unreacted.

β-Elimination. Olefin formation from an adsorbed isobutyl can only occur from β-hydrogen or β-methyl elimination from the isobutyl group. As shown in Eq. [11], α-elimination reactions rapidly lead to complete decomposition of the alkyl and ultimately to carbon atoms on the surface:

$$i\text{-}C_4H_{9,S} \xrightarrow{r_\alpha} C_S \xrightarrow{r_{CO}} CO \qquad [14]$$

These carbon atoms can be oxidized or steam reformed (Eq. [2]) and leave the surface as CO or CO_2 or remain on the surface as coke. As discussed for the oxidative dehydrogenation of other alkanes (9, 10), β-elimination reactions are preferred over α-elimination reactions on the more noble metal surfaces (15–17).

Based on the ratio of hydrogens on 1° carbons to hydrogens on 3° carbons (9 : 1) and the relative strength of these C–H bonds discussed previously, 75% of the isobutyl groups should be adsorbed at the 3° carbon. If the isobutyl group adsorbs on the Pt surface at a tertiary carbon, then the only β-elimination channel available is β-hydrogen elimination to form isobutylene,

$$(CH_3)_3C_S \xrightarrow{r_{\beta 3^\circ}} i\text{-}C_4H_8 + H_S \qquad [15]$$

since there are no β-alkyl groups present. Of course, some fraction of the adsorbed alkyl is undergoing α-scission of the C–C bonds, resulting in propylene, ethylene, or ultimately CO formation (Eq. [14]).

The remaining 25% of the isobutyl groups are adsorbed at a 1° carbon. These species can undergo either β-hydrogen elimination to form isobutylene,

$$(CH_3)_2CHCH_{2,S} \longrightarrow i\text{-}C_4H_8 + H_S \qquad [16]$$

or β-methyl elimination to form propylene,

$$(CH_3)_2CHCH_{2,S} \xrightarrow{r_{\beta 1^\circ}} C_3H_6 + CH_{3,S} \qquad [17]$$

The β-methyl elimination reaction (Eq. [17]) is favored over the β-hydrogen elimination reaction (Eq. [16]) both thermodynamically and statistically. The C–C bond is 21 kcal/mol weaker than the C–H bond (18) and there are two β-methyls compared to only one β-hydrogen. Based on the ratio of β-methyl groups to β-hydrogens (2 : 1) and the relative strength of the C–H and C–C bonds, only 7% of the 1° isobutyl groups will lead to the formation of isobutylene. The rest will go to propylene.

This can be summarized as

$$\begin{aligned} i\text{-}C_4H_{10} &\xrightarrow{75\%} (CH_3)_3C_S \xrightarrow{100\%} i\text{-}C_4H_8 \\ &\xrightarrow{25\%} (CH_3)_2CHCH_{2,S} \xrightarrow{7\%} i\text{-}C_4H_8 \qquad [18] \\ &\qquad\qquad\qquad\qquad \xrightarrow{93\%} C_3H_6, \end{aligned}$$

which shows that with this very simple mechanism we should produce 77% isobutylene and 23% propylene, or three times as much isobutylene as propylene. Under certain experimental conditions, we can obtain these results. Remember, this is an extremely simplified mechanism. We are completely ignoring the contributions of the competing mechanisms and some of these initial products are lost to secondary reactions.

Sequential reactions. In Fig. 7, we expand upon the mechanism described in Eq. [11]. Figure 7 includes the possible reactions of all of the surface adsorbates and lists some of the secondary reactions that take place. Several secondary reactions are not included in Figure 7 but are listed in Table 2, including olefin cracking (Eqs. [9], [10]), CO disproportionation,

$$2CO \rightarrow C_S + CO_2 \qquad [19]$$

and the reverse steam reforming of C_S (Eq. [2]). All of these reactions lead to carbon deposition on the surface.

Not all secondary reactions necessarily involve significant carbon deposition. Once olefins are formed, they can crack to smaller olefins:

$$\begin{aligned} i\text{-}C_4H_8 &\rightarrow C_3H_6 + CH_{2,S} \\ &\rightarrow C_2H_4 + 2CH_{2,S} \end{aligned} \qquad [20]$$

$$C_3H_6 \rightarrow C_2H_4 + CH_{2,S}. \qquad [21]$$

The methylene species formed by these cracking reactions can further crack to C_S and H_S, combine with H_S, and desorb as CH_4, or combine and desorb as C_2H_4.

Also, since there is a significant amount of H_2O present with the products, these olefins are vulnerable to steam reforming:

$$i\text{-}C_4H_8 + 4H_2O \rightarrow 4CO + 8H_2 \qquad [22]$$

$$C_3H_6 + 3H_2O \rightarrow 3CO + 6H_2 \qquad [23]$$

In separate experiments, we have found that the addition of up to 25% H_2O produces no increase in CO, suggesting that steam reforming is not important.

By varying the catalyst contact time, we control the amount of time available for these secondary reactions to take place. As shown in Fig. 4, the isobutylene selectivity decreases with increasing catalyst contact time (decreasing flow rate) but the propylene selectivity remains the same. This suggests that propylene is not lost to secondary reactions (Eqs. [20] and [22]) at a rate comparable to the rate of isobutylene loss (Eqs. [21] and [23]). At the higher flow rates, the isobutylene spends less time in the reaction zone and is less likely to be lost to thermal cracking (Eq. [20]) or steam reforming [Eq. [22]), so the isobutylene selectivity is higher.

Reaction temperature. By increasing the reaction temperature either by preheating the reactants or by reducing the level of N_2 dilution, we greatly improve the isobutane conversion while the isobutylene selectivity remains unchanged and the propylene selectivity increases. By adding heat to the system through diluent removal, the amount of heat that must be supplied by reaction to sustain the autothermal process is reduced. Therefore, more of the less exothermic reactions (Eqs. [1], [5], and [8]), resulting in olefin production, can occur compared to the more exothermic syngas formation reaction (Eq. [7]). With a lower percentage of the oxygen going towards syngas production, there is more available for the dehydrogenation reaction (Eq. [5]), and a higher isobutane conversion results.

At higher temperatures, a larger fraction of the isobutane can react to form isobutylene by oxidative dehydrogenation (Eq. [5]) than must be partially oxidized to form CO. Unfortunately, at these higher temperatures, the rates of the secondary reactions increase. The extra isobutylene produced is thus vulnerable to loss by either thermal cracking to propylene (Eq. [20]) or steam reforming to syngas (Eq. [22]). The combination of these reactions leads to the observed stability in the isobutylene and CO selectivities, while the propylene selectivity increases.

Relative rates. If we assume that all CO and CO_2 are produced through the α-elimination pathway (Eq. [15]), all C_3H_6 is produced from β-methyl elimination from $(CH_3)_2CHCH_{2,S}$ (Eq. [17]), and all isobutylene is produced from β-hydrogen elimination from $(CH_3)_3C_S$ (Eq. [15]), then we can quantify the relative rates of these reactions as shown in Fig. 8. For the purposes of this comparison, we also assume that the secondary reactions are insignificant and no homogeneous reactions occur.

The preference for β-elimination reactions over α-elimination reactions increases at higher fuel/O_2 ratios as the reactant composition moves further from the stoichiometric composition for production of syngas (i-C_4H_{10}/O_2 = 0.5). At higher fuel/O_2 ratios, it appears that the isobutyl group is more apt to adsorb at the 3° carbon atom. At the higher fuel/O_2 ratios, the initial coverage of isobutyl groups is greater. The 3° isobutyl groups may preferentially react given the 1° groups more time to reorient to the thermodynamically favored 3° position, thus increasing the relative production of isobutylene to propylene.

The same trends are observed on both the 5.1 wt.% Pt/α-Al_2O_3 and the 1.8 wt.% Pt/ZrO_2 catalyst. However, the 1.8 wt.% Pt/ZrO_2 catalyst is somewhat less selective to the β-elimination reactions over the α-elimination reac-

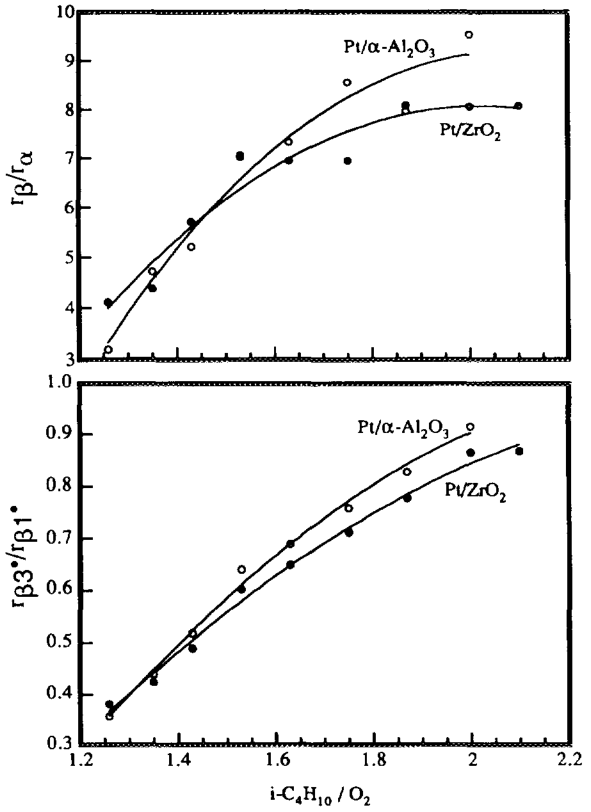

FIG. 8. Comparison of the ratio of the production of β-elimination products (olefins) to α-elimination products (CO and CO_2), r_β/r_α, and the ratio of the production of isobutylene and propylene, $r_{\beta3^\circ}/r_{\beta1^\circ}$, as a function of the fuel/O_2 ratio for a 5.1 wt.% Pt/α-Al_2O_3 catalyst and a 1.8 wt.% Pt/ZrO_2 catalyst. The data shown is for isobutane oxidation in O_2 (20% N_2 diluent) with 360°C preheat at a total flow rate of 5 SLPM at a pressure of 1.4 atm.

tions and slightly less selective to isobutylene production over propylene production. This could be a result of either the support or the Pt loading as will be discussed shortly.

Metal vs oxide. If the metal is present on the support as a film of a nominally uniform thickness, then the higher weight loading catalysts should show fewer characteristics resulting from reactions on the oxide surface. Tables 3 and 4 compare the results for isobutane oxidation over a 5.1 wt.% Pt/α-Al_2O_3, a 1.8 wt.% Pt/ZrO_2, and a 2.6 wt.% Pt/ZrO_2 catalyst. At the lower fuel/O_2 ratio (Table 4), the two ZrO_2 catalysts behave comparably, whereas at the higher fuel/O_2 ratio (Table 3), the 2.6 wt.% Pt/ZrO_2 catalyst behaves much more like the 5.1 wt.% Pt/α-Al_2O_3 catalyst. This suggests that the oxide support contribution to the reactions is more important at the relatively O_2 rich compositions and the metal contribution is more important at the O_2 lean compositions.

When there is more O_2 in the feed, the oxide support (ZrO_2) is more likely to be fully oxidized. Only the fully oxidized oxide catalyst (ZrO_2) has a significant activity for the dehydrogenation of isobutane (Eq. [1]) (7). When less O_2 is present, the oxide is less active and most catalytic reactions take place on the Pt surface as described in the previous sections. When there is sufficient oxygen present to maintain a highly oxidized state in the support, then dehydrogenation reactions occur on the support as well as on the Pt surface. At these lower fuel/O_2 ratios, the higher activity of the ZrO_2 support compared to the α-Al_2O_3 support leads to slightly higher isobutane conversions on the Pt/ZrO_2 catalysts.

That the 2.8 wt.% Au–3.6 wt.% Pt/α-Al_2O_3 catalyst was inactive under these conditions must be explained. The motivation for the investigation of this catalyst lies in the fact that the more noble metals favor β-elimination (olefin formation) reactions over α-elimination (syngas formation) reactions (15, 16). Au is more noble than Pt, so perhaps Au would be a better catalyst than Pt for the selective production of isobutylene. However, Au lacks the catalytic activity required to support this autothermal reaction alone. It was hoped that by combining Pt and Au on the surface, we would obtain a highly active catalyst (like Pt) with less propensity for C–C bond cleavage (like Au).

The complete inactivity of the Pt–Au catalyst suggests that the Au, which was deposited after the Pt, buried the Pt on the surface so that what remained was essentially a Au/α-Al_2O_3 catalyst. Since Au does not catalyze the production of syngas, there was not enough heat generated by exothermic reactions to support endothermic reactions (Eq. [1] and [8]) or even enough energy to cross the activation energy barrier for slightly exothermic reactions (Eq. [5]). Future research will address the effect of catalyst preparation on Pt–Au catalyst activity.

Equilibrium

One of the most striking differences between the results presented here and the work of other research groups on isobutane conversion to isobutylene (1, 2, 7, 8) is the complete absence of catalyst deactivation after several days of operation. Since our residence times are at least 100 times shorter than the residence times of these previous studies, this is equivalent to no coking for >6 months operation at those conditions. At the conditions of these experiments, thermodynamics predicts extensive carbon deposition. If the reactions were reaching equilibrium, carbon deposition would lead to catalyst deactivation. Our experiments are occurring in a much shorter residence time, 5–10 ms, than the other investigations, >300 ms, and we simply are not attaining thermodynamic equilibrium.

There are several reactions that can lead to carbon deposition listed in Table 2, including olefin cracking, CO disproportionation, and reverse steam reforming. The equilibrium constants, K_{eq}, for these reactions, calculated at conditions near the reaction conditions, are listed in Table 2. The experimental values, K_{exp}, of the equilibrium relationships are listed as well; these values are ratios of partial pressures,

$$K_{i\text{-}C_4H_8} = \frac{P_{H_2}^4 a_C}{P_{i\text{-}C_4H_8}} \qquad [24]$$

$$K_{C_3H_6} = \frac{P_{H_2}^3 a_C}{P_{C_3H_6}} \qquad [25]$$

$$K_{C_2H_4} = \frac{P_{H_2}^2 a_C}{P_{C_2H_4}} \qquad [26]$$

$$K_{CO} = \frac{P_{CO} a_C}{P_{CO}^2} \qquad [27]$$

$$K_{H_2O} = \frac{P_{H_2O} a_C}{P_{CO} P_{H_2}}. \qquad [28]$$

For these ratios, we assumed an activity for graphite, a_C, of 1.0.

By comparing the equilibrium constants, K_{eq}, and the experimental equilibrium ratios, K_{exp}, in Table 2, it is apparent that equilibrium is not being obtained. The olefin cracking reactions are not even approaching equilibrium and CO disproportionation and reverse steam reforming are actually being pushed in the reverse direction by thermodynamics.

$$CO_2 + C_S \rightarrow 2CO \qquad [29]$$

$$C_S + H_2O \rightarrow CO + H_2 \qquad [30]$$

It appears that under the nonequilibrium conditions seen here, carbon may be deposited on the surface by olefin cracking, but the CO_2 and H_2O partial pressures are high enough to suppress the coking and remove any carbon that may be present by CO_2 reforming or steam reforming.

CONCLUSIONS

Olefins are produced from isobutane with ~75% selectivity at ~80% isobutane conversion over Pt coated monoliths in an autothermal reactor at atmospheric pressure with a residence time on the order of milliseconds. Isobutylene and propylene are coproduced with similar selectivities. The isobutylene yield of 32% per pass is comparable to the best industrial yield of 45–55% isobutylene, while our total olefin yield far exceeds the industrial maximum. Plus, the reactor discussed here requires a contact time 2–3 orders of magnitude shorter, allowing for a much smaller reactor (lower capital cost), operates autothermally with only minor heat input to boost the conversion (lower production costs), and resists catalyst deactivation (ease of operation).

These results can be explained by a mechanism dominated by heterogeneous reactions. The role of oxygen in this mechanism appears to be that of an initiator. Hydrogen is abstracted by surface oxygen to form an adsorbed isobutyl group and hydroxyl group. Isobutylene is formed from β-hydrogen elimination from an isobutyl group adsorbed at the 3° carbon and propylene is formed from β-methyl elimination from an isobutyl group adsorbed at a 1° carbon.

These reactions may take place on either the Pt surface or the oxide support. The catalytic contribution of the oxide support is significant at lower fuel/O_2 ratios on the Pt/ZrO_2 catalyst where the ZrO_2 is fully oxidized. Under these conditions, the ZrO_2 support has a somewhat higher activity than the α-Al_2O_3 support, leading to a higher isobutane conversion, though the isobutylene selectivity is slightly lower. At higher fuel/O_2 ratios, where the support is oxygen deficient, the catalytic activity of the Pt dominates and no support effects are evident.

The very short contact times and high partial pressures of carbon dioxide and water completely suppress carbon deposition, leading to a long catalyst life. Thus, we obtain high selectivities to olefins at high isobutane conversion under nonequilibrium conditions.

APPENDIX: NOMENCLATURE

a_C	activity of graphite
$K_{C_2H_4}$	experimental equilibrium ratio for ethylene cracking to coke
$K_{C_3H_6}$	experimental equilibrium ratio for propylene cracking to coke
K_{CO}	experimental equilibrium ratio for CO disproportionation
K_{eq}	equilibrium constant
K_{exp}	experimentally calculated equilibrium ratio
K_{H_2O}	experimental equilibrium ratio for the reverse water-gas-shift reaction
$K_{i\text{-}C_4H_8}$	experimental equilibrium ratio for isobutylene cracking to coke
P_i	partial pressure of species i
r_α	rate of all α-scission reactions
r_β	rate of all β-scission reactions
$r_{\beta 1^\circ}$	rate of propylene formation from β-methyl elimination from $(CH_3)_2CHCH_{2,S}$
$r_{\beta 3^\circ}$	rate of isobutylene formation from β-hydrogen elimination from $(CH_3)_3C_S$
r_{CO}	rate of CO formation from C_S
r_{crack}	rate of cracking of olefins to smaller hydrocarbons
r_i	rate of the initiation step

S_i	selectivity to species *i*
Y_i	yield of species *i*
ΔH°	heat of reaction at standard state
ΔT_{ad}	adiabatic temperature rise due to reaction

ACKNOWLEDGMENTS

This research was supported by the NSF under Grant CTS-9311295.

REFERENCES

1. Matsuda, T., Koike, I., Kubo, N., and Kikuchi, E., *Appl. Catal.* **96,** 3 (1993).
2. Zdonik, S. B., *in* "Pyrolysis: Theory and Industrial Practice" (L. F. Albright, B. L. Crynes, and W. H. Corcoran, Eds.) pp. 377–442. Academic Press, New York, 1983.
3. McKay, D. L., and Olbrich, M. E., U. S. Patent 4902849 (to Phillips Petroleum Company), 1990.
4. Olbrich, M. E., McKay, D. L., and Montgomery, D. P., U.S. Patent 4926005 (to Phillips Petroleum Company), 1990.
5. Brinkmeyer, F. M., Savage, K. B., and Bridges, S. D., U.S. Patent 5243122 (to Phillips Petroleum Company), 1993.
6. van Diepen, P. B. J., Veenstra, P., Groeneveld, M. J., Arnoldy, P., Wolff, E. H. P., and Dierickx, J. L. M., E.P. Patent 0561439 A2 (to Shell Internationale Research, Maatschappij, B. V.), 1993.
7. De Rossi, S., Ferraris, G., Freminotti, S., Indovina, V., And Cimino, A., *Appl. Catal. A* **106,** 125 (1993).
8. Takita, Y., Kurosaki, K., Mizuhara, Y., and Ishihara, T., *Chem. Lett.* **2,** 335 (1993).
9. Huff, M., and Schmidt, L. D., *J. Phys. Chem.* **97,** 11815 (1993).
10. Huff, M., and Schmidt, L. D., *J. Catal.* **149,** 127 (1994).
11. Font Freide, J. J. H. M., Howard, M. J., and Lomas, T. A., E.P. Patent 0332289 A2 (to The British Petroleum Company), 1989.
12. Hickman, D. A., and Schmidt, L. D., *J. Catal.* **138,** 267 (1992).
13. Kung, M., Nguyen, K., Patel, D., and Kung, H., *in* "Catalysis of Organic Reactions" (D. Blackburn, Ed.) pp. 289. Dekker, New York, 1990.
14. Burch, R., and Crabb, E. M., *Appl. Catal. A* **100,** 111 (1993).
15. Zaera, F., *Acc. Chem. Res.* **25,** 260 (1992).
16. Jenks, C. J., Chiang, C.-M., and Bent, B. E., *J. Am. Chem. Soc.* **113,** 6308 (1991).
17. Forbes, J. G., and Gellman, A. J., *J. Am. Chem. Soc.* **115,** 6277 (1993).
18. Darabiha, N., Candel, S. M., Giovangigli, V., and Smooke, M. D., *Combust. Sci. Technol.* **60,** 267 (1988).